Chapter 6

VANDUZI MIGMATITE GNEISS

6.1 Introduction

The Vanduzi Migmatite Gneiss occurs between the Messica Granite Gneiss in the west and the Nhansipfe Granitic Orthogneiss in the east (Fig. 2.1) and partially coincides with the zone of anatexis reflected in the 1:250 000 Carta Geologica da Regiao de Vila Manica-Vila Gouveia (1969) and of migmatites (Pinna *et al.*, 1986). Due to the heterogeneous nature of the rock, no chemical analyses were obtained.

6.2 Field Description

The Vanduzi Migmatite Gneiss is bound to the west by the Messica Granite Gneiss and Frontier Formation and to the east by the megacrystic Nhansipfe Granitic Orthogneiss. Field relationships are poorly exposed with the areas underlain by the Vanduzi Migamatite Gneiss showing very subdued topography. In the biotite-hornblende-quartz-feldspar migmatitic gneiss near the Vanduzi river (Fig. 2.2), large scale migmatisation has occurred which is characterized by layers of leucosome which are folded (Fig. 6.1). Two generations of partial melt layers are developed, being the older one folded and parallel to layering in the paleosome (Fig. 6.1).

Figure 6.1: Two generations of partial melting in the Vanduzi Migmatite Gneiss. Note that the second generation partial melt layers transgress the S_1 foliation and leucosomes.

The younger partial melt lenses are oriented N-S and cross-cuts both the planar fabric in the palaeosome and the earlier migmatitic layers (Fig. 6.1). Both generations of partial melt have mafic melanosomes comprising biotite and hornblende. At other localities, mafic boudins may represent interlayered mafic dykes pulled apart during deformation. Near Matsinho, the Vanduzi Migmatite Gneiss consists of more homogeneous biotite-quartz-feldspar gneiss with two generations of migmatisation recognisable in the field. The older leucosomes are recognised by their folded nature and are characterised by biotite-rich melanosomes whereas the younger melt patches are not deformed, share a common orientation, have no biotite-rich melanosome and are characterised by the presence of garnet in the leucosome (Fig. 6.2).

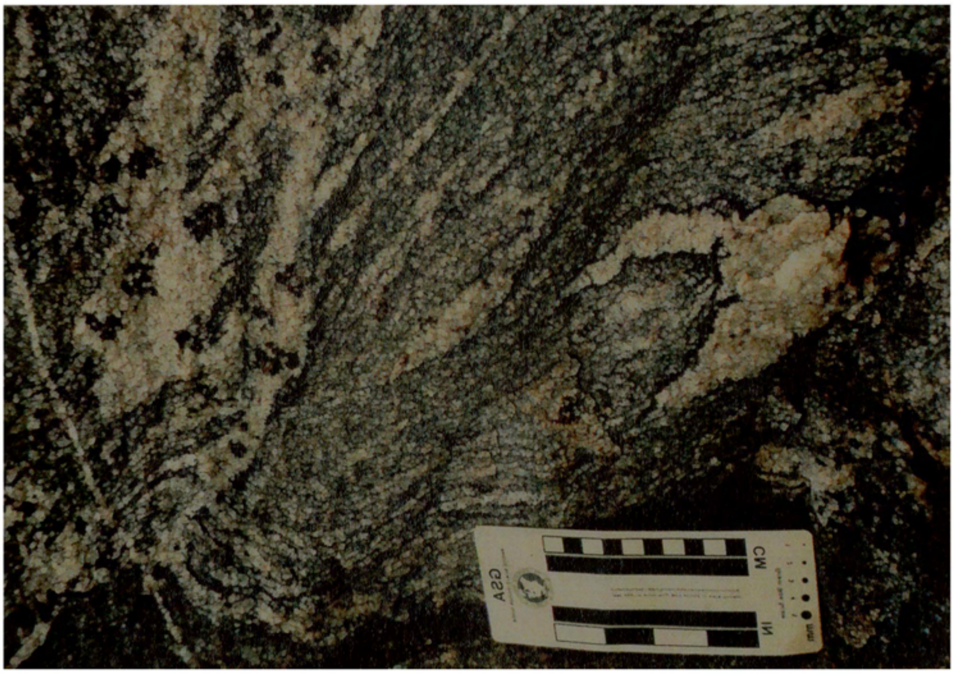

Figure 6.2: First stage stromatic migmatite (right, folded leucosome) and second generation stictolithic migmatite (left leucosomes) near Matsinho. Note garnet grains as part of the partial melt at left.

6.3 Petrography

The mineralogy of the samples is shown in Table 6.1. It is typically granitic being dominated by K-feldspar, plagioclase and quartz with minor amounts of biotite, hornblende and garnet.

The texture of these rocks is typically inequigranular fine- to medium-grained with fine foliated bands of biotite and hornblende interfringed with the granitic leucosome. Locally feldspar and quartz are intergrown to form myrmekite.

Two assemblages are recognized in the samples, namely (1) Plg+Bt+Hbl+K-fld+Qtz and (2) Plg+Bt+Grt+K-fld+Qtz. In assemblage (1) the K-feldspar is microcline, characterized by cross-hatch twinning and minor orthoclase with Carlsbad twinning.

Table 6.1: Mineralogical composition of the Migmatite Gneiss.

samp	K-fld	Plg	Qtz	Bt	Hbl	Ms	Grt	Aln	Ap	Ttn	Opm
mh'gn	35	30	30	4	-	<1	<1	<1	<1	-	-
grR	30	30	30	2	5	-	-	-	-	2	1
nzgg1	32	25	30	5	8	<1	-	<1	<1	<1	<1
mggnv	10	55	25	5	5	<1	-	-	-	-	<1
gr5	45	25	25	3	-	-	1	-	-	-	-

K-fld- potassium feldspar, Qtz- quartz, Plg- plagioclase, Bt- biotite, Hbl- hornblende, Ms- muscovite, Grt- garnet, Aln- allanite, Ttn- titanite, Ap- apatite and Opm- opaque minerals.

The grain size varies from <1-≤2 mm. The plagioclase has a similar grain size, exhibits polysynthetic albite twinning and contains inclusions of quartz, apatite and allanite. Quartz is coarser than the feldspars and has grain sizes varying from >1 to ±2.5 mm and is strained. Biotite is randomly oriented in the granitic leucosome but exhibits preferred orientations in the mafic bands where it defines a foliation together with hornblende. The hornblende is green and locally contains inclusions of quartz, titanite and opaque minerals. Muscovite is rare and commonly occurs as an alteration product of biotite. Allanite is idiomorphic and occurs associated with or as inclusions in plagioclase. Apatite is idiomorphic and occurs as inclusions in plagioclase and hornblende. Titanite is generally associated with hornblende as inclusion in the latter. The samples have low contents of opaque minerals. In assemblage (2) K-feldspar, plagioclase and quartz and the accessory minerals exhibit the same textural characteristics as in (1), but the K-feldspar content is higher leading to overall higher contents of felsic minerals relative to assemblage (1). Biotite occurs randomly in the paleosome and garnet is anhedral and is concentrated in the leucosome.

6.4 Interpretation of Petrography

The mineralogical assemblage of the migmatite gneiss is plotted in a ACF diagram in Figure. 6.3 in which the two mineral associations are distinguishable, namely, (1) Plg+Bt+Hbl+K-fld+Qtz and (2) Plg+Bt+Grt+K-fld+Qtz. The assemblage (1) is typical of mafic- to intermediate igneous rocks whereas the assemblage (2) is typical of semi-pelitic rocks. The association (2) is characterized by a low percentage of ferromagnesian minerals and the occurrence of garnet suggesting that this mineral might have formed by the reaction Bt+Qtz+Ms --->Grt +K-fld+H_2O (in melt).

The combination of granitic bands with bands of biotite and hornblende exhibiting preferred orientation, is typical of migmatites (Pitcher, 1993, p. 238-239) whereby the granitic bands, constituting the leucosome, form as a result of partial melt of feldspars and quartz with the consequent concentration of biotite and hornblende at the margins of these bands. The ferromagnesians (eg. Grt) that are melted or formed in the process are included in the granitic leucosome in which they occur randomly.

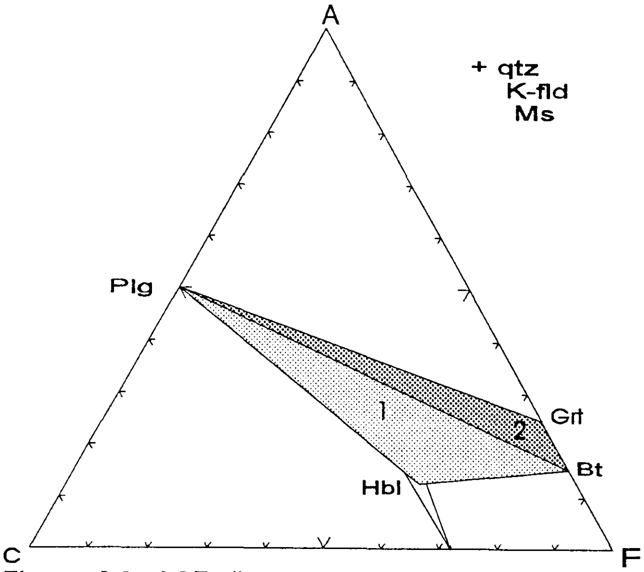

Figure 6.3: ACF diagram of the Vanduzi Migmatite Gneiss mineral assemblage. Plg- plagioclase, K- fld- potassium feldspar, Hbl- hornblende, Grt- garnet Bt- biotite and Ms- muscovite. 1 and 2- reactions as in the main test.

6.5 Leucosome Development History

Migmatites vary in structure from patchy to well layered, stromatic, types (Pitcher, 1993, p. 239). Migmatites are structured into neosome, comprising the newly developed layers of granitic leucosome and melanosome comprising the mafic minerals biotite and hornblende at the margins of the leucosome, and the palaeosome comprising the surviving country rock (Mehnert, 1968, p. 11; Pitcher, 1993, p. 239) (Fig. 6.4).

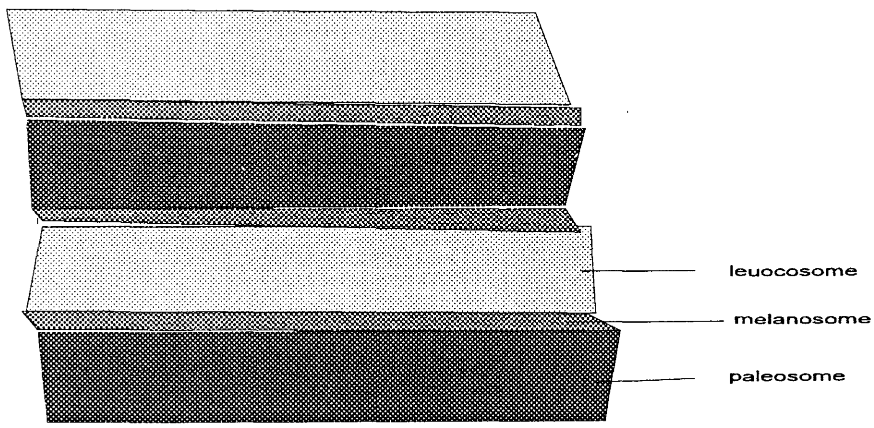

Figure 6.4: Nomenclature of stromatic migmatite (after Mehnert, 1968).

Two types of migmatites are recognized using the classification of Mehnert (1968 p. 18,37) namely stromatic and stictolithic. The stromatic variety is developed in both assemblages (1) and (2) and is characterized by the development of both leucosome and melanosome. The stictolithic variety (flecky gneiss) is only developed in assemblage 2 where the melting reaction of Bt+Qtz+Ms --->Grt+K-fld+H_2O in the melt is considered to have taken place and consequently no melanosome is developed. Both assemblages show two stages of migmatite genesis. Figures 6.1 and 6.2 both show stromatic migmatites characterized by leucosome and melanosome which are deformed. Both figures also show a second generation of migmatization which transgresses the S_1 foliation. In Figure 6.1 the second phase of leucosome development is of a stromatic variety whereas in Figure 6.2 the younger leucosome development is of a stictolithic or flecky gneiss variety.

6.6 Melt P-T Conditions

It is generally accepted that partial melting begins at about 650 °C under pressure of about ≥5 kbar and where $P_{total}=P_{H2O}$ (Pitcher, 1993, p. 239). However, substantial amounts of melt will only be produced as water becomes available from dehydration reactions of minerals and the temperature increases (Mehnert,1987).

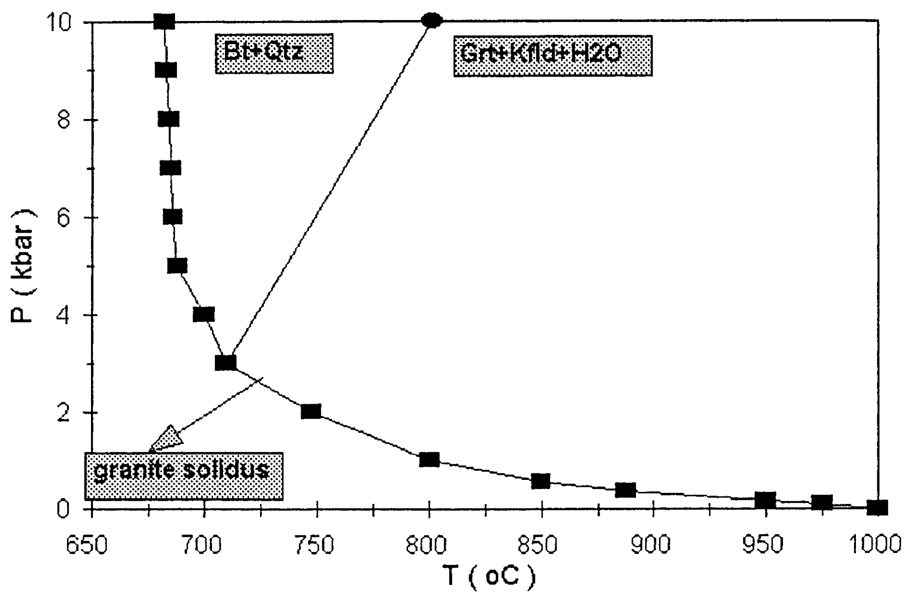

Figure 6.5: Granite solidus for the partial melting during the formation of Vanduzi Migmatitic Gneiss. Solidus data from Ebadi and Johannes (1991) and Johannes and Holtz (1990) and curve redrawn from Johannes, (1985, p. 44).

The structure of the migmatite gneiss near Vanduzi comprises layers of granitic leucosome with mafic selvedges (melanosome) at its margins (Fig. 6.1) suggesting that the melting system did not reach temperatures high enough to melt this mafic phase and incorporate it into the leucosome during first migmatization. These conditions are illustrated by the granite solidus shown in Figure 6.5 for $P_{total}=P_{H2O}$ for a granite with plagioclase >An_{20} (Johannes, 1985). This figure shows that in conditions of minimum temperature melting, only quartzo-feldspatic melts will form the leucosomes whereas in higher temperature garnet may be part of the leucosomes. The occurrence of garnet as part of the leucosome (Fig. 6.2) in assemblage (2) in the migmatite gneiss near Matsinho suggests higher T conditions involving the dehydration melting reaction Bt+Qtz+Ms ---->Grt+K-fld+H_2O (Fig. 6.5).

Chapter 7

CHIMOIO GRANODIORITIC GNEISS

7.1 Introduction

The Chimoio Granodioritic Gneiss underlies the eastern portion of the study area and is named after the town of Chimoio which it underlies. Petrography and geochemistry were conducted on the main body.

7.2 Field Description

The Chimoio Granodioritic Gneiss occurs in the extreme east of the study area (Fig. 2.1) and consists of zones of more homogeneous intermediate biotite-hornblende-quartz-feldspar gneisses interlayered with heterogeneous interlayered amphibolitic and quartzo-feldspathic rocks. The amphibolitic rock is banded and consists of feldspar and quartz (felsic bands) and biotite and hornblende (mafic bands).

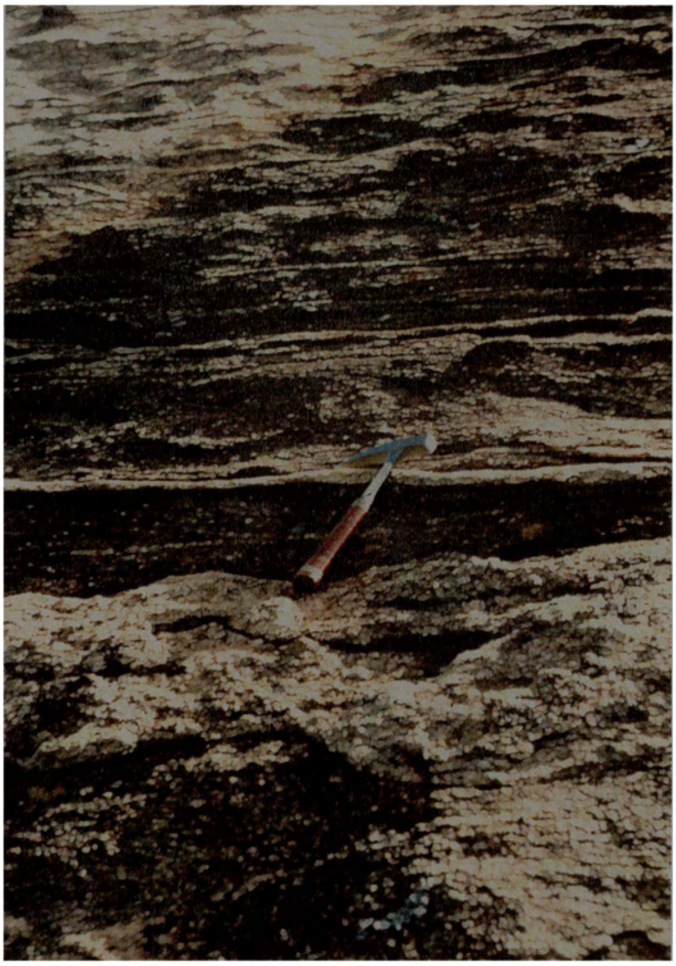

Figure 7.1: Sub-horizontal foliation concordant to the layering in the Chimoio Granodioritic Gneiss.

The migmatization is defined by lenticular layering of granitic partial melt bands oriented N-S with melanosome containing biotite and hornblende. Xenolithic biotite-hornblende rich enclaves are common in the intermediate biotite-hornblende-quartz-feldspar gneisses. The intermediate biotite-hornblende-quartz-feldspar gneisses are characterized by sub-horizontal foliation (Fig. 7.1) whereas in the intercalated amphibolite/leucocratic gneiss the foliation tends to be oriented along a NW-SE strike with steep dips towards the NE. The amphibolite and intercalated gneissic and migmatitic bands are intensely deformed resulting in various type of folds and boudins in the leucosome (Fig. 7.2).

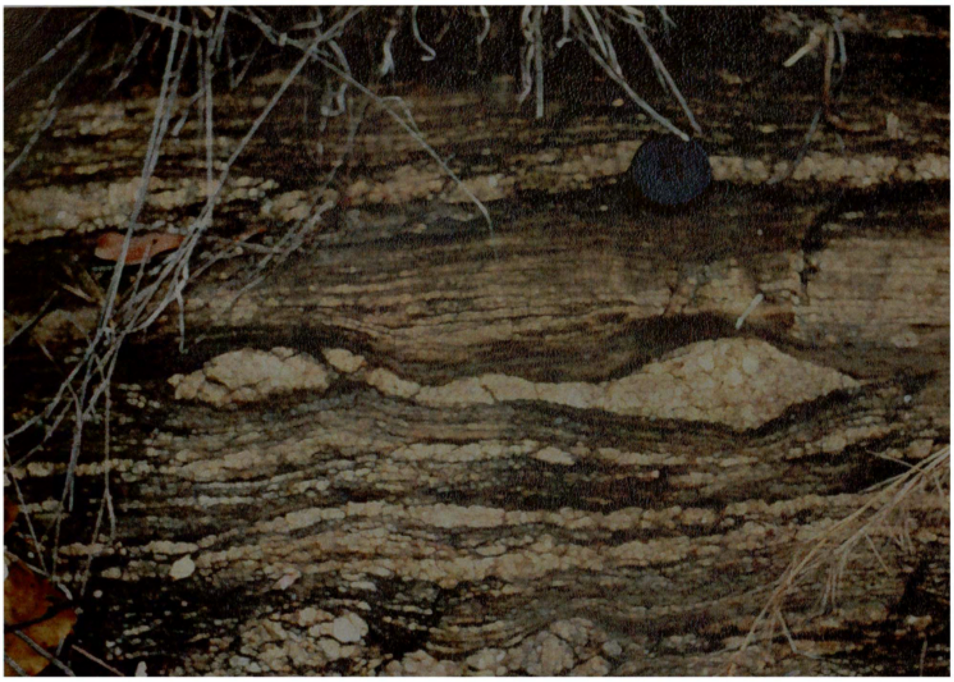

Figure 7.2: Boudinage in the deformed migmatitic gneiss in the Chimoio Granodioritic Gneiss

7.3 Petrography

The mineralogical assemblage of the Chimoio Granodioritic Gneiss consists of plagioclase (48-52%), K-feldspar (20-24%), quartz (8-10%), hornblende (8-12%), biotite (4-8 %) and accessory quantities of opaque minerals, apatite, allanite, muscovite and zircon (Table7.1). The dominant texture is granitic inequigranular medium- to coarse-grained and locally, myrmekites are developed. The samples are poor in quartz and are considerably enriched in hornblende (Fig.7.3) which combined with biotite amounts to a maximum of 22% (Table 7.1).

K-feldspar and plagioclase form equant sub- to anhedral grains exhibiting cross-hatched and Carlsbad and combined Carlsbad-albite twinning respectively. Some grains contain inclusions of fine-grained feldspar, quartz, euhedral apatite and zircon. Some plagioclase grains are unaltered whereas others are cracked and generally sericitized, with cracks filled with sericite and other fine-grained felsic minerals. Quartz is anhedral, strained and locally, some grains enclose fine feldspar and quartz grains.

Table 7.1: Mineral assemblage of Chimoio Granodioritic Gneiss.

samp	K-fld	Plg	Qtz	Bt	Hbl	Ms	Aln	Zrn	Ap	Opm
cvgna	20	51	12	4	10	-	tr	tr	-	2
cvgnb	22	48	10	5	12	-	tr	tr	tr	2
cvgnc	24	51	10	5	8	1	tr	tr	tr	1
cvgnd	20	52	8	5	12	1	-	tr	tr	1
cvgne	22	48	10	8	11	-	tr	-	tr	1
cvgnf	22	50	8	5	12	-	-	tr	tr	3

K-fld- potassium-feldspar, Qtz- quartz, Plg- plagioclase, Bt- biotite, Hbl- hornblende, Ms- muscovite, Aln- allanite, Zrn- zircon, Ap- apatite and Opm- opaque minerals. tr-proportions less than 1%.

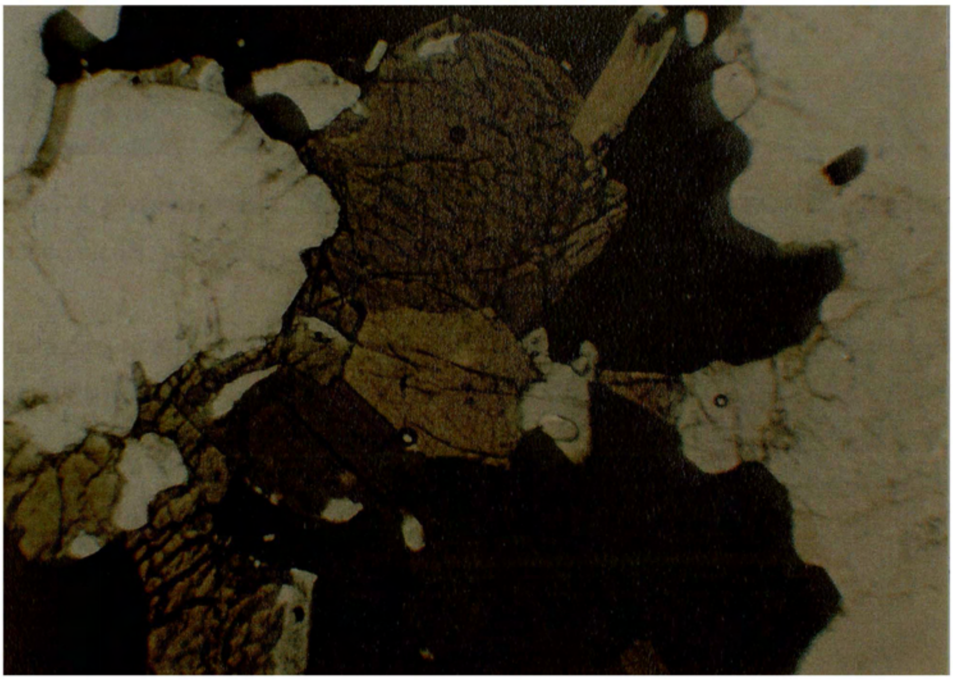

Figure 7.3: Brownish green and buff hornblende, brownish green flakes of biotite and plagioclase (white) in the Chimoio Granodiorite Gneiss. Parallel light, width of field 7 mm.

Finer quartz grains are, in general, unstrained especially those occurring as inclusions. Locally,quartz is intergrown with K-feldspar forming myrmekite (Fig.7.4). Hornblende is poikiloblastic with inclusions of feldspar, quartz, apatite, zircon and allanite. It is subhedral with green to greenish-brown colours, (Fig. 7.3). Biotite occurs as individual grains or aggregates of flakes with straight sides and generally associated with hornblende. It contains inclusions of fine-grained quartz and feldspar. Muscovite is rare and generally occurs as secondary mineral after biotite and plagioclase.

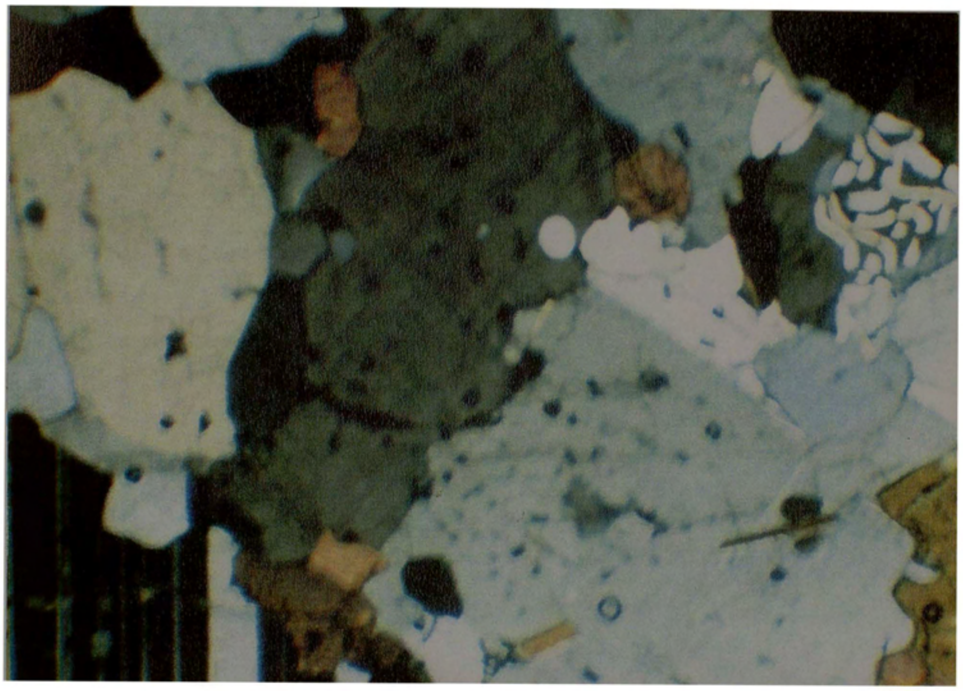

Figure 7.4: Myrmekitic intergrowths (top right) in the gneisses of the Chimoio Granodiritic Gneiss. Crossed nicols, width of field 7 mm.

Allanite occurs as brownish fine grains associated with, or as inclusions in, the ferromagnesian and opaque minerals. When occurring as inclusions, it is commonly euhedral and exhibits concentric zoning. Zircon is short prismatic and is generally enclosed in feldspar and hornblende. Apatite occurs as fine-grained six sided fine grains generally included in feldspar, hornblende and quartz. In addition to these accessory minerals, titanite occurs in trace amounts.

7.3.1 Interpretation of Petrography

The mineralogical assemblage of the Chimoio Granodiorite Gneiss is dominated by plagioclase, K-feldspar , quartz and hornblende as indicated above. The occurrence of hornblende as a metamorphic mineral suggests metamorphism at medium grade amphibolite facies and the plot of this assemblage on an ACF diagram suggests that hornblende, biotite and plagioclase were in equilibrium.

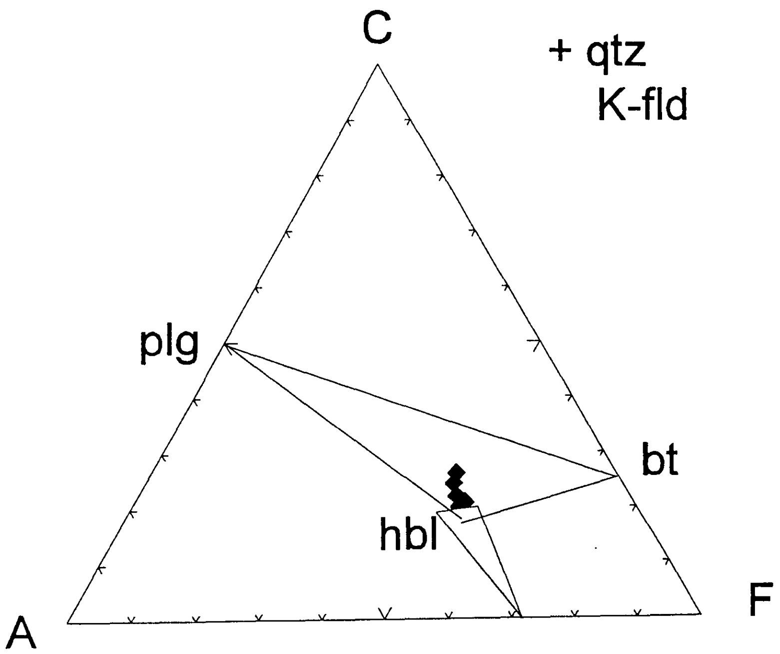

Figure 7.5: ACF diagram showing the equilibrium mineral assemblage of Chimoio Granodioritic Gneiss. Filled squares represent the chemical composition of the samples analysed. plg- Plagioclase, hbl- hornblende, bt- biotite, qtz- quartz and K-feldspar.

7.4 Chemistry

Six samples were analysed for the major and trace elements (Table 7.2) and two samples for the REE (Table 7.3). The same six samples were also subjected to a Rb/Sr isotope study.

7.4.1 Major Element Chemistry

The SiO_2 values do not vary greatly and the contents are intermediate. The samples have similar Al_2O_3 contents. FeO and MgO contents are low and typical of granitoid gneisses. CaO contents are generally greater than both K_2O and Na_2O contents which have similar values. These compositions taken as their equivalent minerals, namely anorthite, K-feldspar and albite, result in the Chimoio gneiss being a granodiorite (Fig. 7.6).

Table 7.2: Major and trace elements and composition A/CNK parameter of the Chimoio Granodioritic Gneiss.

sample	CVGNA	CVGNB	CVGNC	CVGND	CVGNE	CVGNF
SiO2	62.43	58.65	60.89	58.9	58.69	58.81
Al2O3	17.03	16.78	17.97	17.11	17.39	16.47
Fe2O3	2.40	3.20	2.39	3.13	2.94	3.02
FeO	3.22	4.63	3.02	4.42	4.08	4.11
MgO	2.15	2.86	2.12	2.69	2.61	2.68
CaO	4.37	5.82	4.06	5.29	5.34	5.41
Na2O	3.86	3.61	3.76	3.99	3.79	3.95
K2O	3.84	3.63	4.52	3.42	3.79	3.79
TiO2	0.68	0.96	0.72	0.88	0.93	0.92
P2O5	0.32	0.38	0.31	0.38	0.38	0.32
MnO	0.09	0.15	0.09	0.13	0.14	0.13
total	**100.39**	**100.67**	**99.85**	**100.34**	**100.08**	**99.61**
Ba	1851	1813	2016	1318	1685	1735
Li	31	23	32	31	24	24
Nb	10	13	9	13	13	13
Sc	12	17	10	17	14	15
Sr	871	938	820	720	881	913
Rb	104	78	121	95	81	81
Y	23	34	19	33	30	31
Ga	21	23	22	24	21	21
Al	9.02	8.89	9.52	9.06	9.21	8.72
Zr	189	243	177	164	319	245
Y/Nb	2.30	2.62	2.11	2.54	2.31	2.38
A/CNK	0.92	0.82	0.97	0.86	0.87	0.81

Calculation of the parameter Al_2O_3 / $CaO+Na_2O+K_2O$ (Table 7.2) shows that the Chimoio Graonodioritic Gneiss is metaluminous (A/CNK<1 Fig. 7.7). The FeO, MgO, K_2O and Na_2O contents result in the Chimoio Gneiss being typically calc-alkaline in character (Fig. 7.8). TiO_2 and P_2O_5 contents are typical of granitoid gneiss and average 0.9 wt% and 0.34 respectively. A plot of normative quartz (Q), alkali feldspar (A) and plagioclase (P) result in the Chimoio Gneiss being quartz-monzodiorite (Fig. 7.9).

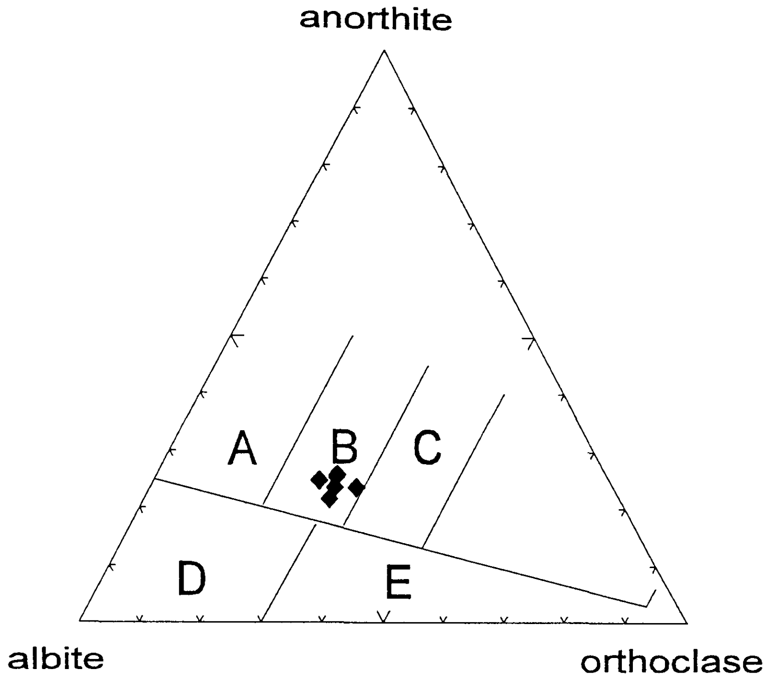

Figure 7.6:Ternary diagram plotting the normative feldspar composition of Chimoio Granodioritic Gneiss. A- tonalite; B-granodiorite; C- Adamelite; D- trondjemite; E- Granite (after Barker,1979).

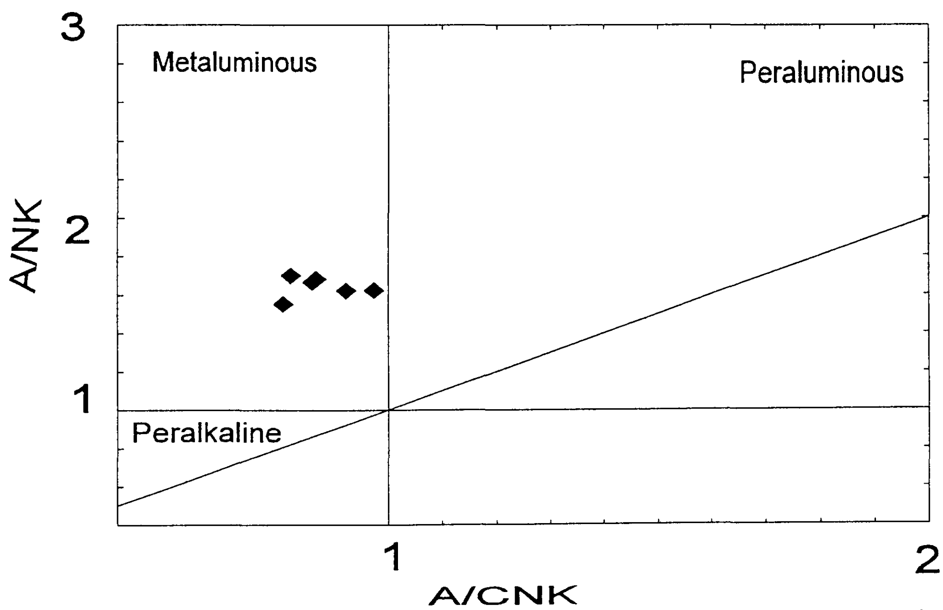

Figure 7.7: Shand's (1947) alumina-saturation diagram plot for the Chimoio Granodioritic Gneiss.

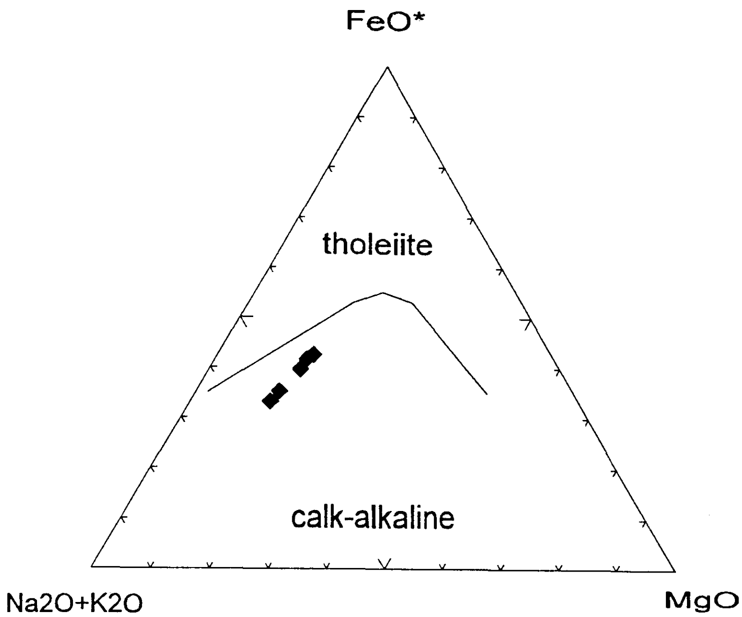

Figure 7.8: Plot of Chimoio gneiss samples into the Irvine and Baragar (1971) diagram for tholeiite and calc-alkaline fields.

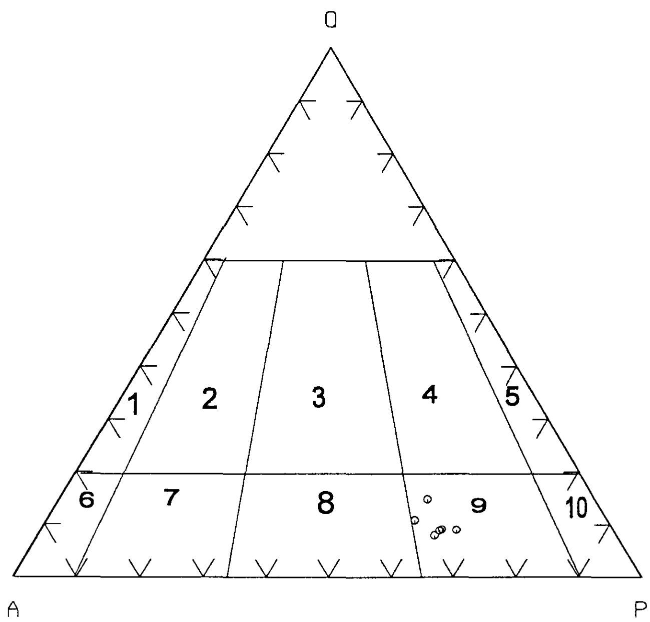

Figure 7.9: Ternary diagram plotting Alkali feldspar (A), plagioclase (P) and quartz (Q) parameters from Chimoio gneiss. Adapted from Streckeisen (1976). 1- alkali feldspar granite; 2- syenogranite; 3- monzogranite; 4- granodiorite; 5- tonalite; 6- quartz alkali feldspar syenite; 7-quartz syenite; 8- quartz monzonite; 9- quartz monzodiorite; 10- quartz diorite.

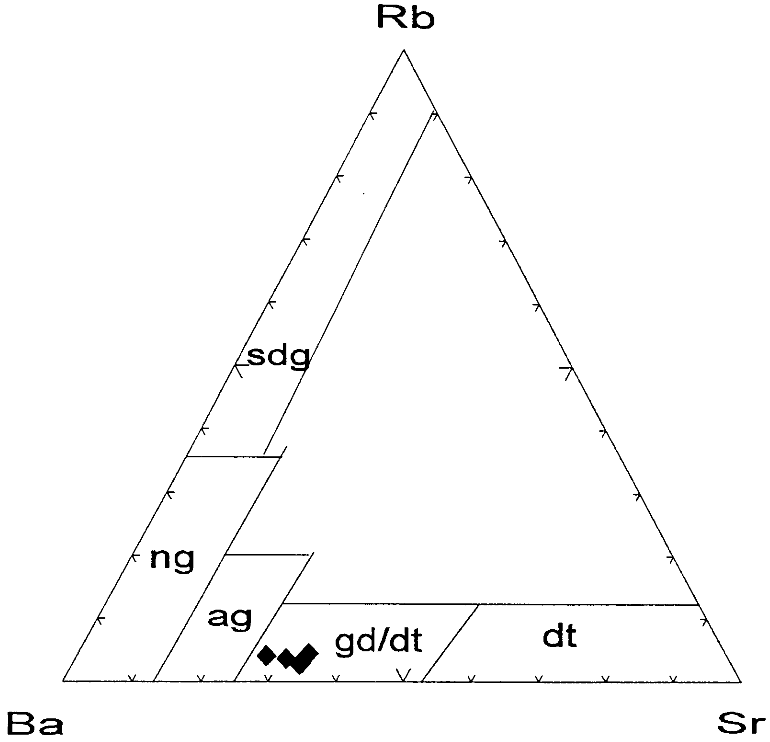

Figure 7.10: Plot of Chimoio Granodioritic Gneiss in the Rb-Ba-Sr diagram (after El Bouseily and El Sokkary (1975). Sdg- strongly differentiated granites; ng- normal granites; ag- anomalous granites; gd/dt- granodiorite and quartz diorite; dt- diorite.

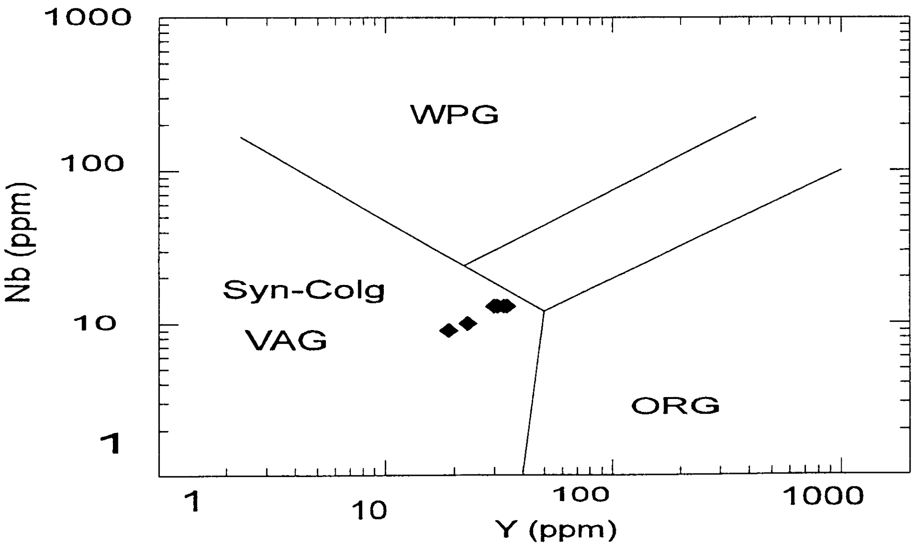

Figure 7.11: Chimoio Granodioritic Gneiss samples plotted into the discriminant diagram for the fields of Within-Plate (WPG), Syn-Collisional (Syn-Colg) and Volcanic - Arc (VAG) and Orogenic (ORG) granitoids (after Pearce *et al.*, 1984).

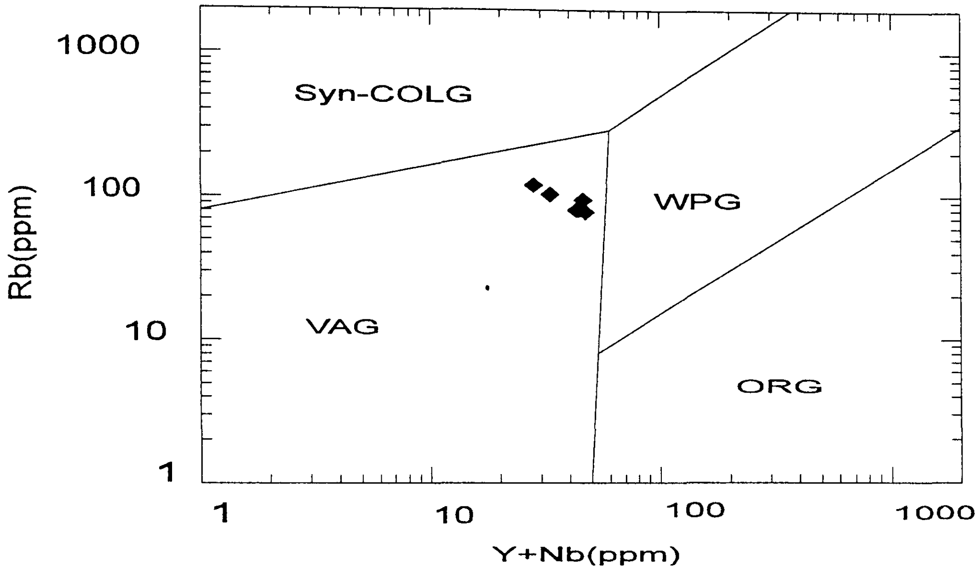

Figure 7.12: Chimoio Granodioritic Gneiss chemical data plotted into the discriminant diagram of Pearce *et al.* (1984). Abbreviation as in Figure 7.11.

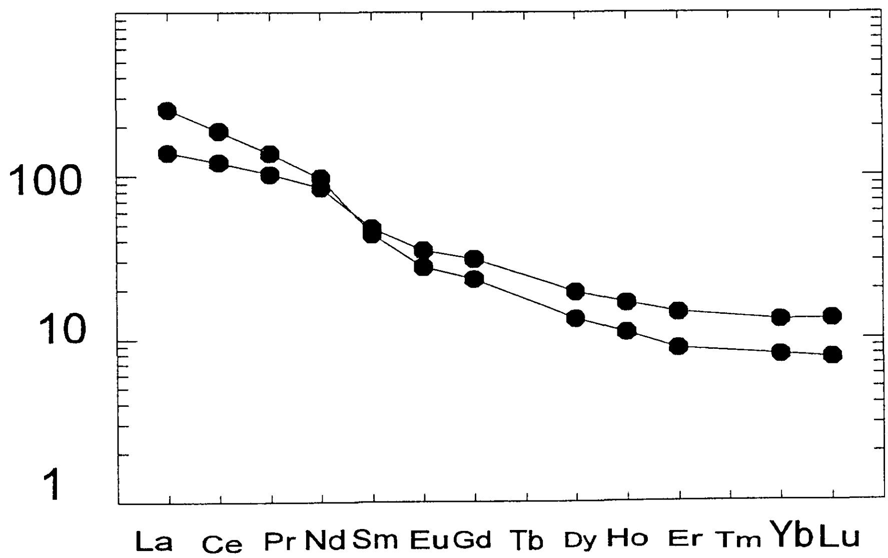

Figure 7.13: REE abundance variation diagram of two samples from Chimoio Granodioritic Gneiss. Normalizing values after Evensen *et al.* (1978).

7.4.2 Trace Element Chemistry

The samples have high Ba and Sr contents but Rb contents are relatively low, a characteristic consistent with the granodioritic nature of the Chimoio granitoids (Fig. 7.10). Sr/Rb ratios are typically 7-10:1 which is consistent with the high plagioclase contents of these gneisses. Zirconium contents are reasonably high and variable. Nb and Y contents are low, a characteristic which is typical of syn-collisional and or volcanic arc granitoids (Fig. 7.11). The Rb, Nb and Y characteristics are typical of volcanic- arc granitoids (Fig. 7.12).

7.4.3 REE Chemistry

The contents of the two samples analysed are shown in Table 7.3 and the chondrite-normalized profiles of samples cvgna and cvgnb are shown in Figure 7.13.

Table 7.3: REE composition of Chimoio Granodioritic Gneiss in ppm.

Sample	La	Ce	Pr	Nd	Sm	Eu	Gd	Dy	Ho	Er	Yb	Lu
CVGNA	62.13	119.9	13.2	46.41	5.78	1.61	4.73	3.37	0.61	1.44	1.27	0.19
CVGNB	33.96	77.34	9.86	40.21	7.41	2.03	5.29	4.9	0.93	2.4	2.08	0.33

The samples have high La_{cn}/Yb_{cn} ratios of about 10:1 resulting in relatively steep REE patterns. The patterns have negligible negative Eu anomalies suggesting that the feldspar fractionation has not played a significant role in the evolution of the gneisses and that plagioclase was not a significant phase in the restitic source of the granitoids.

7.5.4 Radiogenic Rb/Sr Isotope Chemistry

Data of Rb/Sr isotopic study are presented in Table 7.4.

Table 7.4: Radiogenic composition of Chimoio Granodioritic Gneiss.

sample	Rb	Sr	87Rb/86Sr	87Sr/86Sr
cvgna	104	871	0.3523	
cvgnb	78	938	0.2509	0.7105
cvgnc	121	820	0.4088	0.7125
cvgnd	95	720	0.3970	0.71307
cvgne	81	881	0.2694	0.71043
cvgnf	81	913	0.2651	0.7102

Regression of data from the 6 samples using GEODATE (Harmer and Eglington, 1987) using 1.00% and 0.03% errors for the X and Y values respectively yield an errorchron of 1322.22 ± 279 Ma (MSWD 4.995) with $^{87}Sr/^{86}S_i$=0.7054. Exclusion of sample cvgna from the calculation does not materially alter the age or the Ro but results in an isochron of 1236 ± 201Ma (MSWD = 2.221) with Ro=0.7056 (Fig. 7.14). This age places this gneiss between the Messica Granite Gneiss and the Nhansipfe Granitic Orthogneiss to the west.

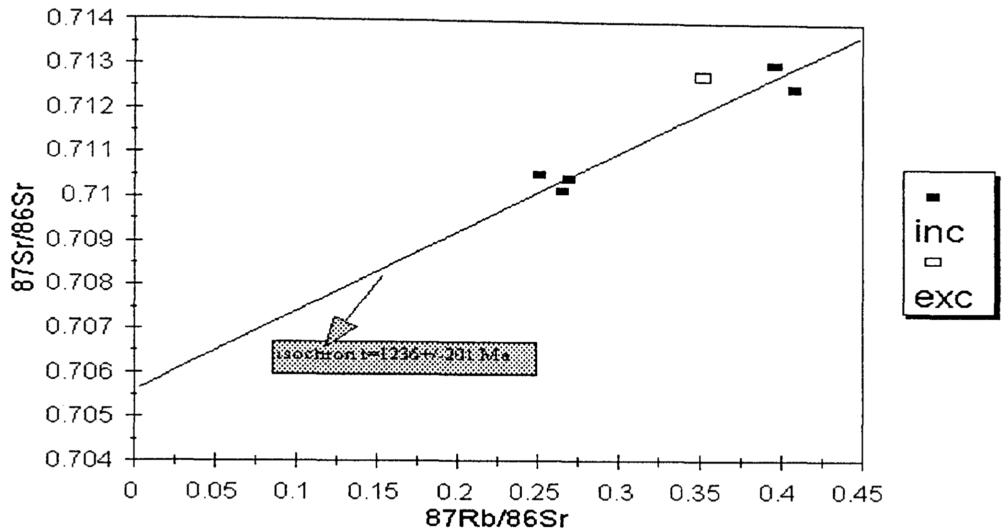

Figure 7.14:Diagram plotting isotopic data of the Chimoio Granodioritic Gneiss. inc indicates included data and exc indicates excluded data.

7.5 Discussion

In Figure 7.6, the Chimoio Granodioritic Gneiss chemical data plot in the field of granodiorite on the basis of feldspar proportions. In this diagram Na_2O, K_2O and CaO are taken as their equivalent minerals albite, orthoclase and anorthite. On the other hand when quartz is taken into account, the gneiss becomes a quartz-monzodiorite, confirming the lower SiO_2 and high CaO nature of this gneiss. Both classifications are acceptable but the granodiorite which is also confirmed by trace elements plot in Figure 7.10 is here preferred. Trace elements chemistry is typical of volcanic-arc granitoids (Fig. 7.12).